

Research report

Morphology of CA3 non-pyramidal cells in the developing rat hippocampus

J.L. Gaiarsa*, I. Khalilov, H. Gozlan, Y. Ben-Ari

IINSERM U29, Avenue de Luminy, B.P. 13, 13273 Marseille Cedex 09, France

Accepted 30 January 2001

Abstract

Although several investigations have shown that the local GABAergic circuit in the rat hippocampus is functional very early in development, this result has not been yet completed by the investigation of the full dendritic and axonal arborization of the neonatal interneurons. In the present study, intracellular injection of biocytin was used to assess the branching pattern of interneurons in the hippocampal CA3 region of rat between 2 and 6 days of age. Based on their dendritic morphology, the biocytin-filled interneurons were divided into four classes: bipolar, stellate, pyramidal-like and fusiform interneurons. About half of the biocytin-filled neonatal interneurons exhibited dendritic or somatic filopodial processes. The axonal arbors of the filled-interneurons were widely spread into the CA3 region, and in four out of nine cases extended beyond the CA3 region to branch into the CA1 region. These results show that, despite immature features, the filopodial processes, the hippocampal interneurons are well developed early in development at a time when their target cells, the pyramidal neurons, are still developing. These observations are consistent with a trophic role that GABA may play early in development. © 2001 Elsevier Science B.V. All rights reserved.

Theme: Development and regeneration

Topic: Pattern formation

Keywords: Biocytin; GABA; Interneuron; Hippocampus; Development

1. Introduction

Neurons in the hippocampal formation can be classified into principal cells, i.e. pyramidal and granule cells, and non-principal cells, i.e. interneurons. While they form only 10–15% of the total cell population, the interneurons exhibited a great heterogeneity in terms of morphological features, electrophysiological properties, and peptide or calcium-binding protein contents (for review see [11]). In spite of this heterogeneity, most of the hippocampal interneurons are thought to use γ -aminobutyric acid (GABA) as neurotransmitter (for review see [35]).

Given the crucial role played by GABAergic interneurons in shaping population activity of principal cells [8,9,24,36] several studies have investigated the functional

maturation of GABAergic synapses. These studies have shown that GABAergic synaptic transmission dominates at early stages of development in the rat hippocampus. Thus, GABAergic cells are generated before birth, earlier than principal cells [2,37]. At embryonic stages, GABAergic cells are transiently located within two layers, and from the third postnatal day of life they appear throughout the whole hippocampus [30]. As early as at postnatal (P) day 1, GAD-positive processes are found in the dendritic region of the principal cells, whereas few are observed in the principal cell body layer [10]. At P5, GABAergic cells form synaptic contact on principal cells, providing the morphological substrate of inhibition in the neonatal hippocampus [32,33]. More recently, it was shown that GABAergic and glutamatergic synaptic transmissions are established sequentially with GABAergic synapses being functional before glutamatergic synapses on CA1 hippocampal pyramidal cells [40]. Moreover, electrophysiological [19] studies have shown that interneurons are functionally integrated into the neonatal hippocampal

*Corresponding author. Tel.: +33-4-9182-8129; fax: +33-4-9182-8100.

E-mail address: gaiarsa@inmed.univ-mrs.fr (J.L. Gaiarsa).

network, where they provide most of the spontaneous synchronous activity (reviewed in [5]).

Although these observations show that the local GABAergic circuit within the hippocampal formation is established and functional very early in development, this result has not been yet completed by an investigation of the full dendritic and axonal arborization of the neonatal interneurons. In previous studies, Golgi technique was used to investigate the morphology of developing hippocampal interneurons [21,26]. This technique however does not allow the visualisation of the full dendritic and axonal arbors. In the present study interneurons were intracellularly filled with the marker biocytin during recordings from 350 μm thick rat hippocampal slices, providing a good assessment of dendritic and axonal arbors. The results show that, despite immature features such as the presence of spine-like or filopodial processes on both soma and dendrites, the neonatal hippocampal interneurons exhibited a well developed dendritic tree, and a widely distributed axonal arbor extending to the whole CA3 region.

2. Materials and methods

2.1. Slice preparation

Experiments were performed on hippocampal slices obtained from postnatal day (P) two to six male Wistar rats. Brains were removed under ether anaesthesia and submerged in cold (0°C) artificial cerebrospinal fluid (ACSF) of the following composition (in mM): NaCl, 126; KCl, 3.5; CaCl_2 , 1.3; MgCl_2 , 1.3; NaH_2PO_4 , 1.2; NaHCO_3 , 25; and glucose, 11; pH 7.4 when equilibrated with 95% O_2 /5% CO_2 . Hippocampal slices (350 μm thick) were cut on a vibratome (FTB Vibracut). The slices then recovered for at least 1 h in ACSF at room temperature (20 – 23°C), and were transferred individually in a submerged recording chamber (flow rate of 4 ml ACSF/min at 34°C).

2.2. Intracellular labelling

We used the patch-clamp technique (whole cell configuration) to load the interneurons with biocytin. The composition of the pipette solution was the following: K-gluconate (135 mM), CaCl_2 (0.1 mM), Mg-ATP (2 mM), ethylene glycol-bis (B-aminoethyl ether)-*N,N,N,N* tetraacetic acid (EGTA) (1 mM) and *N*-2-hydroxyethylpiperazine-*N*-2-ethanesulfonic acid (HEPES) (10 mM) and biocytin (1%); pH=7.2. CA3 interneurons were patched under visual control (Zeiss Axioscope, $\times 40$ water immersion objective) at the surface or not more than 50 μm depth. Only interneurons having a resting membrane potential more negative than -40 mV were selected.

2.3. Tissue processing and morphological analysis

After injection, the slices were incubated for 30 to 60 min at room temperature in ACSF. The slices were then fixed overnight at 4°C in 1% paraformaldehyde and 1% glutaraldehyde in phosphate buffer (PB, 0.1 M, pH=7.4) and transferred in sucrose 30% PB solution. Following several rinsing in phosphate buffer saline (PBS, 0.02 M, pH=7.4), the slices were treated with Triton X-100 (0.3% in PBS) for 30 min and incubated for 4 h in avidin (Molecular Probes) diluted in PBS (1:800). After rinsing in PBS, the slices were incubated for 4 h in biotin-horseradish peroxidase (Molecular Probes) diluted in PBS (1:800). Following several rinsing in Tris-HCl (0.05 M, pH=7.6) the slices were reacted with diaminobenzidine (DAB, 50 mg/100 ml Tris-HCl) and H_2O_2 (0.01%) for 20 min to visualise the injected cells. The slices were then rinsed in Tris-HCl, dehydrated in graded ethanol, cleared with xylene and mounted in Eukit. The labelled interneurons were drawn with the aid of a $\times 25$ or $\times 100$ oil immersion objectives and a camera lucida attachment.

3. Results

Interneurons of the rat hippocampal CA3 region were intracellularly loaded with biocytin between postnatal day (P) 2 to 6. At that stage of development, all interneurons recorded in the present study exhibited spontaneous synaptic activity mediated by ionotropic GABAergic and glutamatergic receptors and, as already reported [19], were characterised by the presence of spontaneous periodical large inward currents (data not shown). Cells were considered well filled when the staining was uniform throughout the dendritic and axonal arbors. Since the interneurons were patched at the surface or not more than at 50 μm depth, only interneurons with an obvious complete dendritic tree were selected. 13 labelled-interneurons met these criteria and were included in the present study.

3.1. Interneurons classification

The biocytin-filled interneurons were classified as bipolar (Fig. 1, cells 1–3) or multipolar (Fig. 1, cells 4–13) based on the number and distribution of their primary dendrites. The soma of the bipolar interneurons was located in the stratum radiatum, and their dendrites confined therein except for cell 1 (Fig. 1) with one dendritic branch entering the pyramidal layer. The general orientation of the bipolar interneurons was parallel to the pyramidal layer. The multipolar interneurons were further subclassified into stellate (Fig. 1, cells 4–8), pyramidal-like (Fig. 1, cells 9–11) and fusiform (Fig. 1, cells 12 and 13) interneurons. The soma and dendrites of three stellate interneurons were located in the stratum radiatum (Fig. 1, cells 4, 5 and 8). The soma of the two remaining stellate

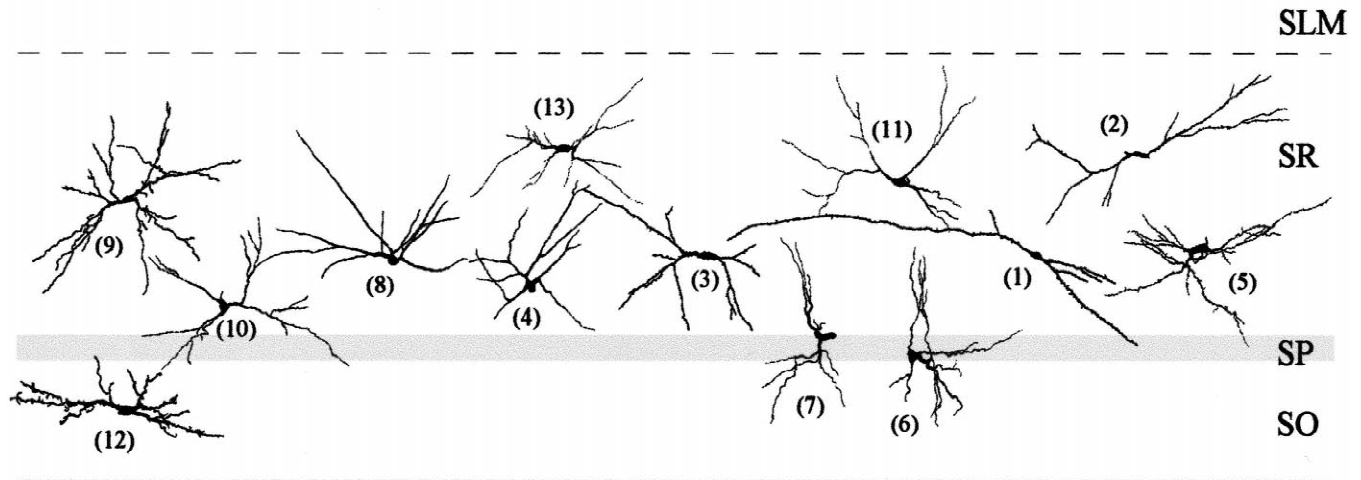


Fig. 1. Composite drawings of the dendritic arbors of interneurons stained with intracellular injection of biocytin. Original camera lucida drawings were used, with slight modifications to obtain the best fit for all cells. The laminar distribution of the dendrites has been preserved. Abbreviation for this and subsequent figures: SO: stratum oriens; SP: stratum pyramidale; SR: stratum radiatum; SLM: stratum lacunosum moleculare.

interneurons were located into the pyramidal layer (Fig. 1, cells 6 and 7). The soma of pyramidal-like interneurons was located in the stratum radiatum (Fig. 1, cells 9–11). Their dendrites ramified throughout the stratum radiatum and were confined therein, except for the cell 10 (Fig. 1) with two descending dendrites entering the pyramidal layer. One fusiform interneurone was located into the stratum oriens (Fig. 1, cell 12) and the other into the stratum radiatum (Fig. 1, cell 13). Their dendrites were oriented horizontally parallel to the pyramidal layer and restricted to the same stratum as the cell body.

About half of the biocytin-labelled interneurons (6 out of 13) exhibited spine-like or filopodial processes on their dendrites (cells 1, 2, 3, 5, 10 and 11), or cell bodies (cells 3 and 11). These spine-like processes appeared thin and elongated (Fig. 2, A–C) and differed in density and shape from cell to cell. Some interneurons also displayed dendritic swelling (Fig. 2D).

3.1.1. Axonal arbor

A limitation inherent to slice preparation is that the axons and dendrites were cut when preparing slices. Therefore among the 13 labelled-interneurons, only nine interneurons were considered successfully stained to investigate the axonal arbor. For the other interneurons, the amount of axon recovered was insufficient as several collaterals were seen to leave the slice.

3.1.1.1. Stratum oriens fusiform interneurone. Fig. 3 shows a camera lucida reconstruction of the dendritic and axonal arbors of a fusiform interneurone labelled at P2 with the cell body and dendrites confined to the stratum oriens. Three main dendrites emerged from the ovoid cell body, and extended for a distance of 250 μm parallel to the CA3 pyramidal layer. This cell exhibited a total dendritic

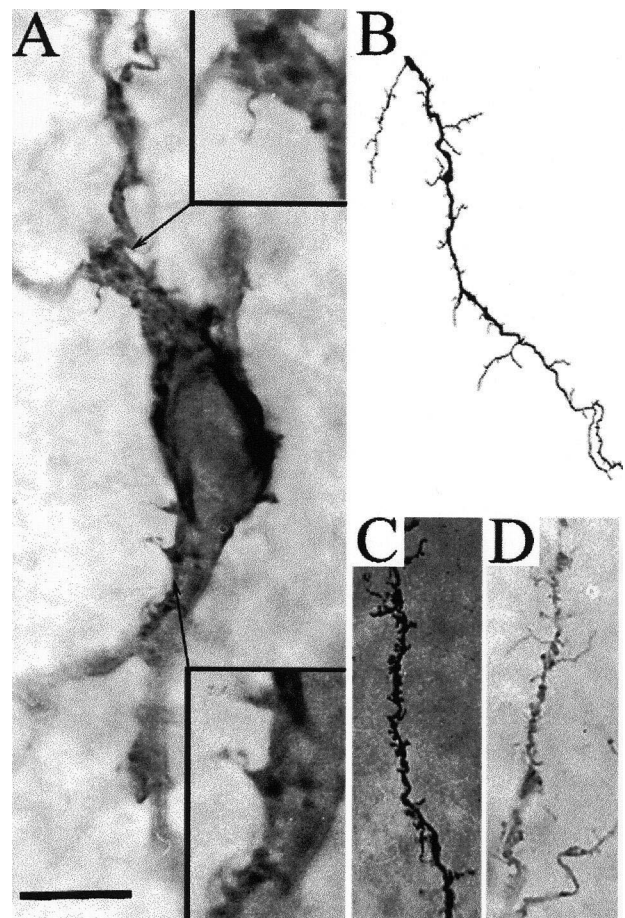


Fig. 2. Photomicrograph showing the presence of spine-like processes or filopodia on the soma (A) and dendrites (B–D) of stained neonatal hippocampal interneurons. Scale bar 10 μm .

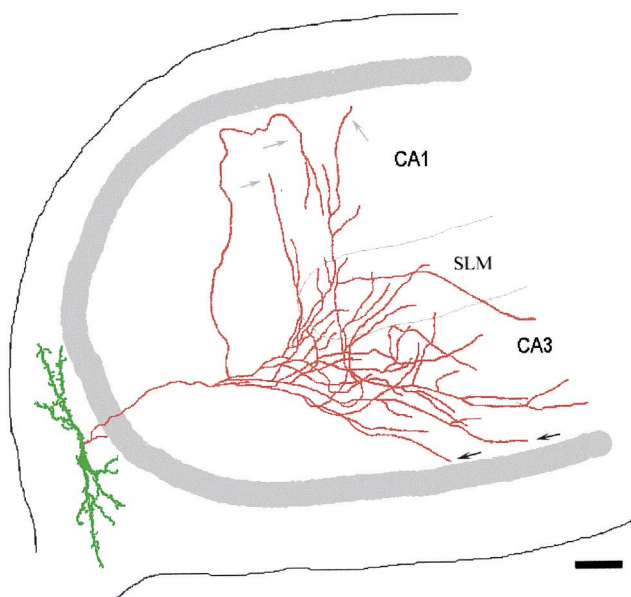


Fig. 3. Camera lucida reconstruction of the dendritic (green) and axonal (red) arborization of a biocytin-filled interneurons at P2. In this and subsequent figures the pyramidal layer is indicated by a thick grey line. The soma and dendrites were located in the stratum oriens and covered by thin spine-like processes. This interneurone was classified as fusiform. The axon ramified into the CA3 stratum radiatum. Some collaterals entered the SLM or the CA1 SR (grey arrows). Other collaterals entered the CA3 stratum lucidum (black arrows). Scale bar 50 μm .

length of 1200 μm and eight dendritic branching points. The secondary dendrites were covered by elongated filopodial processes (see Fig. 2A and D). The axon arose from the proximal part of a primary dendrite, and ascended from the stratum oriens directly to the stratum radiatum where it gave off several collaterals. These collaterals ran mainly parallel to the CA3 pyramidal layer into the stratum radiatum and stratum lacunosum moleculare towards the dentate gyrus. Some collaterals entered into the stratum lucidum in a close apposition with the pyramidal layer (Fig. 3, black arrows) or into the CA1 region towards the pyramidal layer (Fig. 3, grey arrows).

3.1.1.2. Bipolar interneurons. Fig. 4 shows the complete axonal and dendritic reconstruction of tree bipolar interneurons stained at P6 (Fig. 4A) and P3 (Fig. 4B and C). Two main dendrites emerged from the opposite pole of the soma and extended for a distance of 600 μm (Fig. 4A), 150 μm (Fig. 4B) and 250 μm (Fig. 4C) into the stratum radiatum. These cells exhibited four (Fig. 4A), seven (Fig. 4B) and nine (Fig. 4C) dendritic branching points, and their total dendritic length was 700 μm (Fig. 4A), 400 μm (Fig. 4B) and 625 μm (Fig. 4C). The soma (Fig. 4B) and dendrites (Fig. 4A–C) were covered by thin filamentous spine-like processes. Shortly after emerging from the proximal part of a primary dendritic branch, the axon of the cell depicted in Fig. 4A gave off numerous collaterals into the stratum radiatum that ran towards the dentate

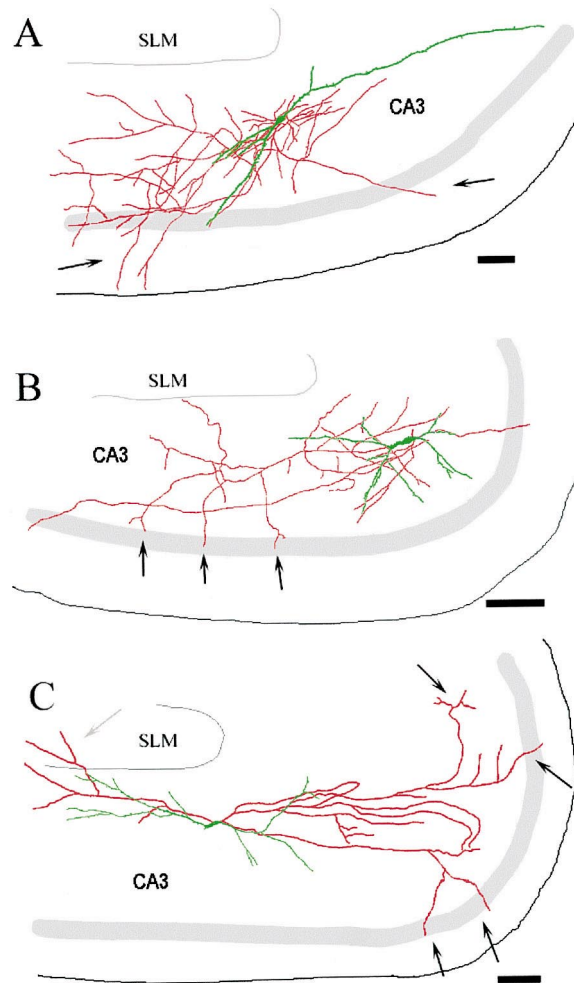


Fig. 4. Camera lucida reconstruction of the dendritic (green) and axonal (red) arborization of bipolar interneurons stained at P6 (A) and P3 (B and C). Their soma and dendrites were confined to the stratum radiatum. The axonal arbor ramified into the stratum radiatum and some collaterals entered the stratum oriens (black arrows). Scale bars: 50 μm .

gyrus. Some collaterals were seen to enter into the stratum oriens (Fig. 4A, black arrows). Extensive thin and varicose axon collaterals also spread radially in the vicinity of the cell body. The axon of the cells depicted in Fig. 4B,C arose from the cell body and rapidly ramified within the stratum radiatum to give off collaterals towards the dentate gyrus (Fig. 4B) or the fimbria (Fig. 4C). Some collaterals were found to terminate near or within the pyramidal layer (Fig. 4B–C, black arrows) or to enter into the SLM (Fig. 4C, grey arrow).

3.1.1.3. Pyramidal-like interneurons. Fig. 5 illustrates tree examples of stratum radiatum pyramidal-like interneurons stained at P4 (Fig. 5A), P3 (Fig. 5B) and P5 (Fig. 5C). These cells exhibited a total dendritic length of 1550 μm (Fig. 5A), 1250 μm (Fig. 5B) and 1200 μm (Fig. 5C). The total number of dendritic branching points was eight for the cells in Fig. 5A and 5B, and 10 for the cell in Fig. 5C. Both soma and dendritic trees were smooth, except for

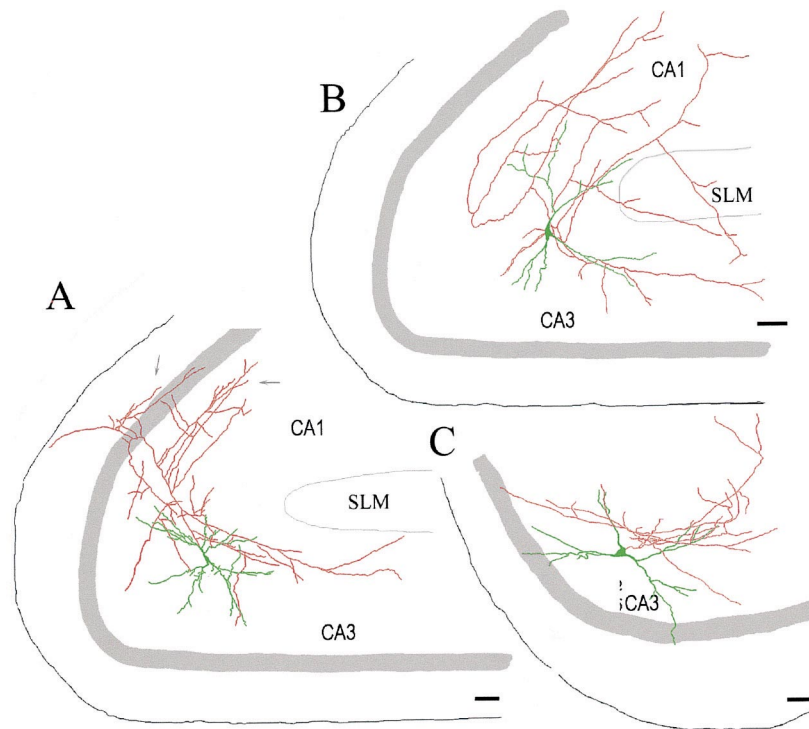


Fig. 5. Camera lucida reconstruction of the dendritic (green) and axonal (red) arborization of pyramidal-like interneurons stained at P4 (A), P3 (B) and P5 (C). Their soma and dendrites were confined to the stratum radiatum, except for the cell depicted in C, with dendrites entering the stratum oriens. The axonal arbor ramified into the stratum radiatum. The cell depicted in A exhibited a bistratified axonal arbor (grey arrows). Scale bars: 50 μm .

the interneurone in Fig. 5B, that exhibited thin spine-like processes along the secondary dendrites. The axonal arbor of these interneurons differed from each other. The axon of the interneurone depicted in Fig. 5A arose from the cell body and ran toward the stratum radiatum of the CA1 region. Along his course, it gave off numerous axonal branches. Some of them turn toward the dentate gyrus into the stratum radiatum of the CA3 region (Fig. 5A). Within the CA1 region, the axonal network appeared bistratified, with collaterals running parallel to the pyramidal layer in the strata radiatum and oriens (Fig. 5A, grey arrows). The axonal network of the interneurone in Fig. 5B also ramified into the CA1 and CA3 but was restricted to the upper part of stratum radiatum. Some axonal branches emerging in the CA1 region crossed the SLM to invade the CA3 region. The axonal network of the interneurone in Fig. 5C was less spread. Shortly after emerging from the cell body, the axon branched in several collaterals restricted to the CA3 stratum radiatum mainly directed toward the dentate gyrus.

3.1.1.4. Stellate interneurons. Fig. 6 illustrates two examples of stellate interneurons stained at P3. The cell body of these interneurons were located into the CA3 stratum radiatum and the dendrites were confined therein. These cells exhibited eight dendritic branching points and a total dendritic length of 1200 μm (Fig. 6A) and 1100 μm (Fig. 6B) respectively. Both cells were aspiny. The axon of

these cells arose from the cell body and rapidly branched to give off several collaterals that had a predominantly radial orientation. The axonal network was mainly confined to the stratum radiatum of the CA3 region toward the dentate gyrus (Fig. 6A) or the CA1 region (Fig. 6B). Several collaterals were found in a close apposition of the CA3 (Fig. 6A, black arrow) or CA1 (Fig. 6B, black arrow) pyramidal layer or to invade the stratum oriens (Fig. 6A–B, grey arrows).

4. Discussion

Our results, based on the reconstruction of neonatal rat hippocampal interneurons intracellularly filled with the marker biocytin, provides a complex image of their morphology with both immature and more adult-like features. Thus, interneurons exhibit spine-like processes or filopodia on both soma and dendrites that will disappear subsequently. Their dendrites and axonal arbors are well developed with a degree of extension that will enable to a wide control of the electrical activity that GABAergic interneurons exert at this early stage [4].

4.1. Immature features

One feature frequently encountered in the present study was the presence of long and thin spine-like processes or

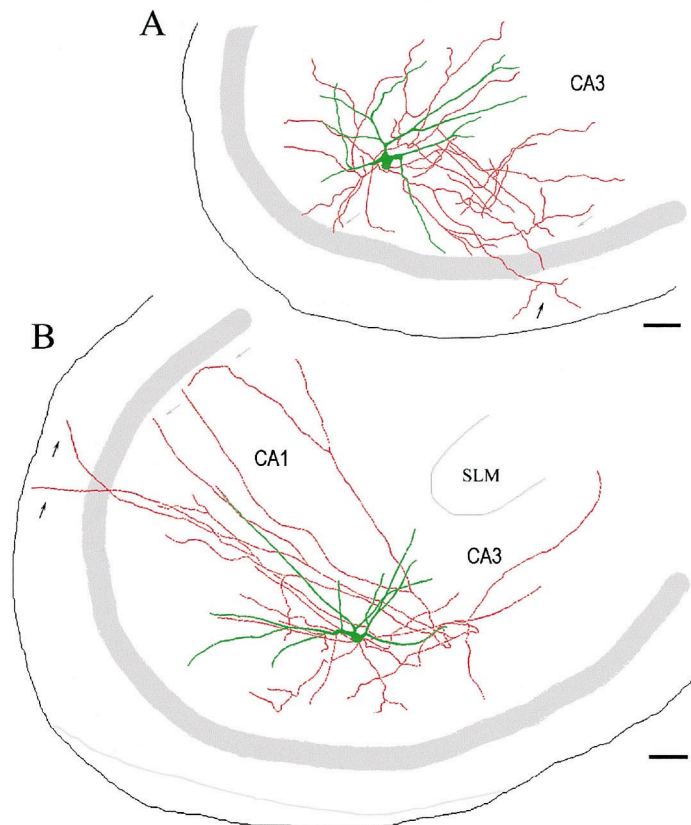


Fig. 6. Camera lucida reconstruction of the dendritic (green) and axonal (red) arborization of two stellate interneurons stained at P3. Their soma and dendrites were confined to the stratum radiatum, but axonal arbor ramified into the stratum radiatum, but collaterals entered the CA3 (A) or CA1 (B) stratum oriens (grey arrows). Other collaterals terminated in a close apposition of the CA3 (A) or CA1 (B) pyramidal layer (black arrows). Scale bars: 50 μ m.

filopodia on both soma and dendrites of neonatal hippocampal interneurons. While their density, shape and length varied from cell to cell, they were present on about half of the labelled interneurons. Similar dendritic and somatic thin processes were observed on fusiform basket interneurons in the rat dentate gyrus during the first postnatal week of life [31] and on neonatal Golgi-stained neocortical interneurons [25]. These thin processes may represent immature features of neonatal interneurons. Thus, most, but not all [1,16,38], adult interneurons display beaded and smooth dendrites [7,17,20,23,27]. In addition, the spines-like processes originating from neonatal interneurons are clearly different from regular, short spines observed on adult neurons, but rather resemble the already reported filopodial spines [29].

4.2. Dendritic and axonal arbors of neonatal hippocampal interneurons

A limitation inherent to slice preparation is that the axons and dendrites were cut, and therefore the labelled interneurons were probably incomplete. In spite of this limitation, our study suggests that the dendritic tree of neonatal interneurons is well developed and appears far

more extensive than the adjacent CA3 pyramidal neurons [12]. Our staining also shows that the axonal arbors of most neonatal interneurons cover the entire width of the CA3 stratum radiatum, with collaterals entering the stratum lacunosum moleculare, the pyramidal layer, the stratum oriens or both. In addition, the axonal collaterals of four out of nine labelled-interneurons were seen to project to both CA3 and CA1 regions, while description of adult [6,17,18,39,41] and pups [14] interneurons demonstrated only few of such collaterals in CA1 area but instead a remarkable target specificity in the placement of their synaptic contacts.

A comparison with adult is complicated by the fact that interneurons represent an extremely heterogeneous population [11,28]. The above observation however suggests that some types of neonatal CA3 interneurons will undergo axonal remodelling as development progresses. For instance, the interneuron 12 (Fig. 4) labelled in the present study, with soma and dendrites confined to the stratum oriens resemble the already described O-LM interneurons [17,23,34]. The axon of this cell type in adult ascends from the soma directly to the stratum lacunosum moleculare to form a dense cloud of collaterals. The neonatal interneuron 12 also sends axon collaterals toward the stratum

lacunosum moleculare, but additional collaterals entered the stratum radiatum of both CA1 and CA3 region. Therefore, we suggest that some types of interneurons undergo axonal remodelling as reported for CA3 pyramidal cells [15] and dentate-gyrus basket cells [31].

4.3. Physiological relevance

The interneurons stained in the present study exhibited both GABAergic and glutamatergic spontaneous synaptic activities showing that they were functionally integrated into the developing hippocampal network. Because 90% of the hippocampal interneurons located within the strata oriens and radiatum are immuno-reactive for GABA or GAD [42], the neonatal loaded-interneurons are likely GABAergic interneurons. In previous studies it was shown that GABAergic interneurons provide most of the synaptic drive on neonatal CA3 pyramidal cells [5,13] and may exert a trophic action on the neuritic growth of hippocampal neurons [3,22]. According to these observations, we found that the dendritic and axonal arbors of neonatal interneurons are extensive at a time when the pyramidal cells, are still developing [12]. Thus, GABAergic interneurons are in a unique position to influence the functional and morphological development of their target cells.

Acknowledgements

This work was supported by the Institut National de la Santé et de la Recherche Médicale.

References

- [1] D.G. Amaral, A Golgi study of the cell types in the hilar region of the hippocampus in the rat, *J. Comp. Neurol.* 182 (1978) 851–894.
- [2] D.G. Amaral, J. Kurz, The time of origin of cells demonstrating glutamic acid decarboxylase-like immunoreactivity in the hippocampal formation of the rat, *Neurosci. Lett.* 59 (1985) 33–39.
- [3] G. Barbin, H. Pollard, J.-L. Gaiarsa, Y. Ben-Ari, Involvement of GABA_A receptors in the outgrowth of cultured hippocampal neurons, *Neurosci. Lett.* 152 (1993) 150–154.
- [4] Y. Ben-Ari, E. Cherubini, R. Corradetti, J.-L. Gaiarsa, Giant synaptic potentials in immature rat CA3 hippocampal neurons, *J. Physiol. (Lond.)* 416 (1989) 303–325.
- [5] Y. Ben-Ari, R. Khazipov, X. Leinekugel, O. Caillard, J.-L. Gaiarsa, GABA_A, NMDA and AMPA receptors: a developmentally regulated 'ménage à trois', *Trends Neurosci.* 20 (1997) 523–529.
- [6] E.H. Buhl, K. Halasy, P. Somogyi, Diverse sources of hippocampal unitary inhibitory postsynaptic potentials and the number of synaptic release sites, *Nature* 368 (1994) 823–828.
- [7] E.H. Buhl, Z.S. Han, Z. Lörinczi, V.V. Stezhka, S.V. Karnup, P. Somogyi, Physiological properties of anatomically identified axo-axonic cells in the rat hippocampus, *J. Neurophysiol.* 71 (1994) 1289–1307.
- [8] G. Buzsáki, M. Penttonen, Z. Nadasdy, A. Bragin, Pattern and inhibition-dependent invasion of pyramidal cell dendrites by fast spikes in the hippocampus in vivo, *Proc. Natl. Acad. Sci. U.S.A.* 93 (1996) 9921–9925.
- [9] S.R. Cobb, E.H. Buhl, K. Halasy, O. Paulsen, P. Somogyi, Synchronization of neuronal activity in hippocampus by individual GABAergic interneurons, *Nature* 378 (1995) 75–78.
- [10] S.T. Dupuy, C.R. Houser, Prominent expression of two forms of glutamate decarboxylase in the embryonic and early postnatal rat hippocampal formation, *J. Neurosci.* 16 (1996) 6919–6932.
- [11] T.F. Freund, G. Buzsáki, Interneurons of the hippocampus, *Hippocampus* 6 (1996) 347–470.
- [12] J.-L. Gaiarsa, M. Beaudoin, Y. Ben-Ari, Effect of neonatal degranulation on the morphological development of rat CA3 pyramidal neurons: Inductive role of mossy fibers on the formation of thorny excrescences, *J. Comp. Neurol.* 321 (1992) 612–625.
- [13] J.-L. Gaiarsa, H.A. McLean, P. Congar, X. Leinekugel, R. Khazipov, V. Tseeb, Y. Ben-Ari, Postnatal maturation of gamma-aminobutyric acid_A and _B-mediated inhibition in the CA3 hippocampal region of the rat, *J. Neurobiol.* 26 (1995) 339–349.
- [14] C.M. Gomez-Di Cesare, K.L. Smith, F.L. Rice, J.W. Swann, Anatomical properties of fast spiking cells that initiate synchronized population discharges in immature hippocampus, *Neuroscience* 75 (1996) 83–97.
- [15] C.C. Gomez-Di, K.L. Smith, F.L. Rice, J.W. Swann, Axonal remodeling during postnatal maturation of CA3 hippocampal pyramidal neurons, *J. Comp. Neurol.* 384 (1997) 165–180.
- [16] A.I. Gulyas, R. Miettinen, D.M. Jacobowitz, T.F. Freund, Calretinin is present in non-pyramidal cells of rat hippocampus-I. a new type of neuron specifically associated with the mossy fibre system, *Neuroscience* 48 (1992) 1–27.
- [17] A.I. Gulyas, R. Miles, N. Hajos, T.F. Freund, Precision and variability in postsynaptic target selection of inhibitory cells in the hippocampal CA3 region, *Eur. J. Neurosci.* 5 (1993) 1729–1751.
- [18] A.I. Gulyas, R. Miles, A. Sik, K. Toth, N. Tamamaki, T.F. Freund, Hippocampal pyramidal cells excite inhibitory neurons through a single release site, *Nature* 366 (1993) 683–687.
- [19] R. Khazipov, X. Leinekugel, I. Khalilov, J.-L. Gaiarsa, Y. Ben-Ari, Synchronization of GABAergic interneuronal network in CA3 subfield of neonatal rat hippocampal slices, *J. Physiol. (Lond.)* 498 (1997) 763–772.
- [20] J.C. Lacaille, P.A. Schwartzkroin, Stratum lacunosum-moleculare interneurons of hippocampal CA1 region. II. intrasomatic and intradendritic recordings of local circuit synaptic interactions, *J. Neurosci.* 8 (1988) 1411–1424.
- [21] U. Lang, M. Frotscher, Postnatal development of nonpyramidal neurons in the rat hippocampus (areas CA1 and CA3): a combined Golgi/electron microscope study, *Anat. Embryol. (Berl.)* 181 (1990) 533–545.
- [22] X. Leinekugel, I. Medina, I. Khalilov, Y. Ben-Ari, R. Khazipov, Ca²⁺ oscillations mediated by the synergistic excitatory actions of GABA_A and NMDA receptors in the neonatal hippocampus, *Neuron* 18 (1997) 243–255.
- [23] G. Maccaferri, J.D.B. Roberts, P. Szucs, C.A. Cottingham, P. Somogyi, Cell surface domain specific postsynaptic currents evoked by identified GABAergic neurons in rat hippocampus in vitro, *J. Physiol. (Lond.)* 524.1 (2000) 91–116.
- [24] R. Miles, K. Toth, A.I. Gulyás, N. Hájos, T.F. Freund, Differences between somatic and dendritic inhibition in the hippocampus, *Neuron* 16 (1996) 815–823.
- [25] M.W. Miller, Development of projection and local circuit neurons in the neocortex, in: A. Peters, E.G. Jones (Eds.), *Development and Maturation of Cerebral Cortex*, Plenum Press, New York, 1999, pp. 133–175.
- [26] H.G. Minkwitz, Zur Entwicklung der Neuronenstruktur des Hippocampus während des prä- und postnatalen ontogenese des Albinoratte, *J. Hirnforsch.* 17 (1976) 233–253.
- [27] U. Misgeld, M. Frotscher, Postsynaptic-GABAergic inhibition of non-pyramidal neurons in the guinea-pig hippocampus, *Neuroscience* 19 (1986) 193–206.

- [28] P. Parra, A.I. Gulyas, R. Miles, How many subtypes of inhibitory cells in the hippocampus?, *Neuron* 20 (1998) 983–993.
- [29] C.E. Riback, L. Seress, D.G. Amaral, The development, ultrastructure and synaptic connections of the mossy cells of the dentate gyrus, *J. Comp. Neurol.* 14 (1985) 835–857.
- [30] F. Rozenberg, O. Robain, L. Jardin, Y. Ben-Ari, Distribution of GABAergic neurons in late fetal and early postnatal rat hippocampus, *Dev. Brain Res.* 50 (1989) 177–187.
- [31] S.L. Seay-Lowe, B.J. Claiborne, Morphology of intracellularly labeled interneurons in the dentate gyrus of the immature rat, *J. Comp. Neurol.* 324 (1992) 23–36.
- [32] L. Seress, M. Frotscher, C.E. Riback, Local circuit neurons in both the dentate gyrus and Ammon's horn establish synaptic connections with principal neurons in five days old rats: a morphological basis for inhibition in early development, *Exp. Brain Res.* 78 (1989) 1–9.
- [33] L. Seress, C.E. Ribak, Postnatal development of the light and electron microscopic features of basket cells in the hippocampal dentate gyrus of the rat, *Anat. Embryol. (Berl.)* 181 (1990) 547–565.
- [34] A. Sik, M. Penttonen, A. Ylinen, G. Buzsaki, Hippocampal CA1 interneurons: an in vivo intracellular labeling study, *J. Neurosci.* 15 (1995) 6651–6665.
- [35] L. Sivilotti, A. Nistri, GABA receptor mechanisms in the central nervous system, *Prog. Neurobiol.* 36 (1991) 35–92.
- [36] I. Soltesz, D.K. Smetters, I. Mody, Tonic inhibition originates from synapses close to the soma, *Neuron* 14 (1995) 1273–1283.
- [37] E. Soriano, A. Cobas, A. Fairen, Asynchronism in the neurogenesis of GABAergic and non-GABAergic neurons in the mouse hippocampus, *Dev. Brain Res.* 30 (1986) 88–92.
- [38] E. Soriano, M. Frotscher, Spiny nonpyramidal neurons in the CA3 region of the rat hippocampus are Glutamate-like immunoreactive and receive convergent mossy fiber input, *J. Comp. Neurol.* 332 (1993) 435–448.
- [39] N. Spruston, J. Lübke, M. Frotscher, Interneurons in the stratum lucidum of the rat hippocampus: An anatomical and electrophysiological characterization, *J. Comp. Neurol.* 385 (1997) 427–440.
- [40] R. Tyzio, A. Represa, I. Jorquera, Y. Ben-Ari, H. Gozlan, L. Aniksztejn, The establishment of GABAergic and glutamatergic synapses on CA1 pyramidal neurons is sequential and correlates with the development of the apical dendrite, *J. Neurosci.* 19 (1999) 10372–10382.
- [41] I. Vida, M. Frotscher, A hippocampal interneuron associated with the mossy fiber system, *Proc. Natl. Acad. Sci. U.S.A.* 97 (2000) 1275–1280.
- [42] W. Woodson, L. Nitecka, Y. Ben-Ari, Organization of the GABAergic system in the rat hippocampal formation: a quantitative immunocytochemical study, *J. Comp. Neurol.* 280 (1989) 254–271.